Hierarchical Bandwidth Phase Modulation for Reduced Peak-to-Average Power Ratio in Ultrabroadband Terahertz Communications

Duschia M. Bodet and Josep Miquel Jornet

Ultrabroadband Nanonetworking Laboratory
Department of Electrical and Computer Engineering
Institute for the Wireless Internet of Things
Northeastern University, Boston, MA, USA
E-mail: {bodet.d,jmjornet}@northeastern.edu

***Abstract*—Hierarchical Bandwidth Modulations (HBMs) have been proposed to leverage the distance-dependent bandwidth of terahertz (THz) communication systems and allow single-transmitter multiple-receiver (STMR) systems to support users with different data rate requirements at the same time and frequency and in the same direction. HBM has much potential for purposes of multiplexing users, maximizing the overall system data rate, and accommodating each receiver's channel. Up until now, HBM has been explored using quadrature and amplitude modulations. However, given the non-linearity of THz transmitters, modulations with high peak-to-average power ratios (PAPRs) are discouraged. In this paper, phase-only HBM is proposed, with the goal of solving the PAPR problem. In particular, after defining the key parameters affecting the performance of HBM using phase shift keying (PSK) constellations, an optimal constellation design is derived. The solution is numerically and experimentally tested and benchmarked. The results show the potential of PSK-HBM as a solution for THz communications to increase the data rate without increasing the PAPR.**

***Index Terms*—Terahertz communications; 6G; Hierarchical Modulations; Experimental Research**

I. Introduction

The terahertz band (0.1 – 10 THz) is predicted to be key in fulfilling the increasing demand for wireless systems [1]. A growing number of THz-communication systems are being designed and tested within the research community [2]. Now, with the allocation of bands in the tens of GHz in the fifth generation (5G) of cellular networks, THz communication systems are that much closer to becoming a reality in industry.

One of the known challenges of THz communications is the high path loss suffered by signals in the THz band. High frequencies correspond to small wavelengths that lead to very small antenna footprints resulting in high propagation losses. Moreover, molecular absorption at certain resonance frequencies within the THz band result in additional losses which cause the available bandwidths to depend on the transmission distance [3]. Many hardware solutions have been proposed to combat these losses; namely, highly directional antennas [2], large multiple-input multiple-output (MIMO) systems [4], intelligent reflective surfaces (IRS)s [5]. These hardware solutions are promising, but there has been little consideration on how we might engineer the waveform itself to overcome or even leverage these high losses at THz frequencies. Hierarchical Bandwidth Modulation (HBM) first proposed in [6] and expanded upon in [7] provides an approach to exploiting the high propagation and absorption losses in the THz band by engineering the signal waveform itself.

A novel modulation technique, HBM allows transmitters to simultaneously serve multiple users at different symbol rates corresponding to each user's available bandwidth. It was shown to outperform traditional hierarchical modulations (HM) and time sharing techniques, and HBM was proven to successfully exploit the available bandwidth in the THz band [6] [7]. Thus far, HBM has only been considered using a hierarchical quadrature amplitude modulation (QAM) constellation, but THz-communication systems that exist today have non-linear transmitters struggle to modulate signals with high Peak-to-Average-Power Ratios (PAPRs) [2]. Since the QAM constellations explored for HBM in [6] can have high PAPRs, in this paper we present HBM with a hierarchical Phase Shift Keying (PSK) constellation.

In this paper, we make the following contributions:

- Design the constellation and derive expressions for the error rate of a HBM PSK systems
- Explore the functional region for defining a successful HBM PSK system
- Provide first experimental results of HBM PSK in the THz band to verify its feasibility
- Analyze the performance of HBM QAM and PSK systems to show that the HBM PSK scheme offers a viable solutin for PAPR-sensitive broadband communications

The rest of this work is organized as follows. In Sec. II we describe HBM PSK and the modulator and demodulator structure. Next, in Sec. III, we derive the performance of the HBM PSK system, verify the performance with simulations, and explore the functional region as an important consideration in the design of HBM PSK. We compare the QAM and PSK performance in Sec. IV before giving our experimental results are given in Sec. V. We conclude this work in Sec. VI.

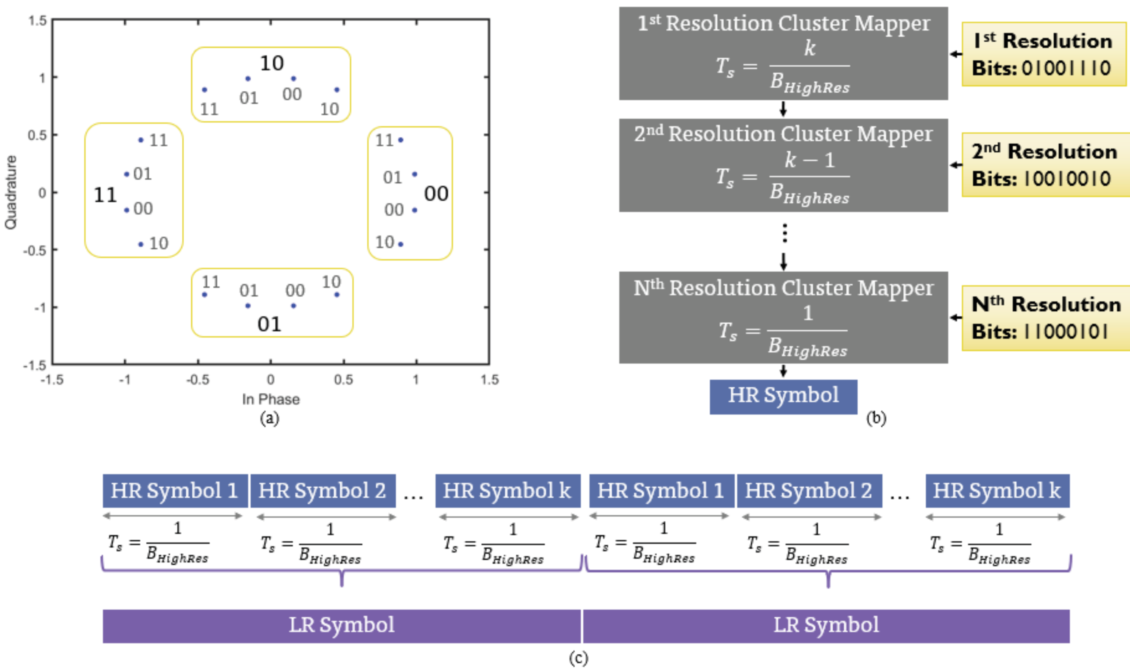

Fig. 1. HBM PSK constellation and modulator structure showing low resolution (LR) and high resolution (HR) symbols

II. Hierarchical Bandwidth Modulations

HBM is a hierarchical modulation scheme in which some receivers demodulate information at a faster symbol rate than others. The concept of changing the symbol rate with multi-resolution constellations is an innovative solution not explored before [6]. Fig. 1 describes the HBM PSK modulator. Notice how Fig. 1a and Fig. 1b demonstrate a simultaneous hierarchy in the constellation while Fig. 1c demonstrates HBM's hierarchical nature with respect to symbol duration (i.e. bandwidth). In traditional HM schemes described in [8] the resolutions only exist in the constellation, and a receiver's SNR alone determines which resolution can be used. For HBM, however, the bandwidth used for each receiver also determines the resolution. Thus receivers demodulating the higher orders of the constellation receive information at a faster symbol rate than receivers demodulating lower orders of the constellation. For example, if a receiver that is close to the transmitter receives the high resolution (HR) symbols at a rate of R_s, a receiver that is farther away would receive the low resolution (LR) symbols at a rate of R_s/k, where k is a positive integer as shown in Fig. 1c. Notice in Fig. 1c that the LR symbols are a sequential combination of k HR symbols. In order for this scheme to work, the k HR symbols within the same LR symbol must all exist in the same cluster of the hierarchical constellation in Fig. 1a. The LR bits determine which cluster to use, and the HR bits determine which point within that cluster is modulated. Thus for the 2-level resolution case, there are two separate bitstreams of information. The LR stream is received by both users corresponding to the yellow boxes (i.e. clusters) of the hierarchical constellation.

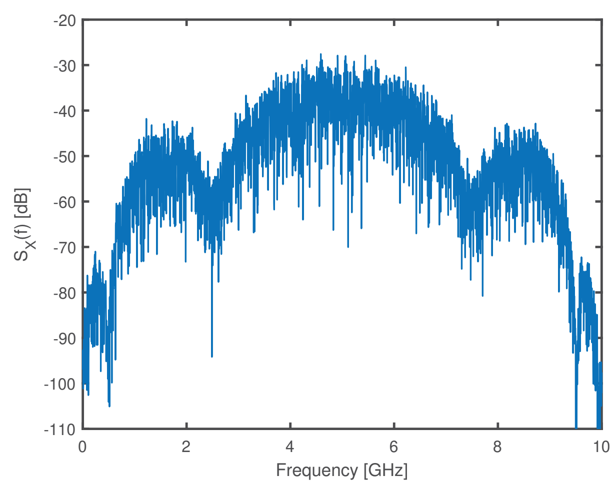

Fig. 2. The frequency spectrum of a 2-resolution HBM system.

The HR stream corresponds to the individual constellation points within each cluster shown in blue. This is implemented by the the modulator structure shown in Fig. 1b. Each block of the modulator corresponds to a level of resolution in the PSK constellation. In the 2-level example shown in Fig. 1a, the first cluster mapper would map two bits from its bitstream to one of the four clusters. The second cluster mapper would take two bits from its bitstream and map to the corresponding constellation point within the cluster.

Because HBM is hierarchical in terms of the constellation *and* in terms of bandwidth, this first bitstream with the LR information can be fully decoded from the main lobe of the signal spectrum shown in Fig. 2. All receivers would observe this main lobe toe detect the information corresponding to the LR clusters shown by the yellow boxes in Fig. 1a. The second level information exists in both the main lobe as well as the two side lobes of spectrum. It corresponds to the individual blue constellation points shown in Fig. 1a. A receiver that is far away from the transmitter in the THz channel would either not observe these side lobes because the absorption loss would filter them out or opt to demodulate at the LR to reduce the observed noise and filter out the side lobes itself.

III. Characterizing Performance of HBM PSK Systems

In this section we begin by defining key parameters and deriving the symbol error rate (SER) for the 2-level HBM PSK constellation. After verifying the expression with simulations we proceed to use it to define the HBM functional region for the PSK system.

A. SER Calculation

Considering a two-level resolution, Fig. 3 shows the parameters defining the constellation. $2\phi_1$ is the angle between the centers of the LR clusters and can be given by

$$2\phi_1 = \frac{2\pi}{M_{LR}}, \tag{1}$$

where M_{LR} is the modulation order of the LR constellation ($M_{LR} = 4$ in Fig. 3). Similarly, M_{HR} is defined as the modulation order of the non-uniform HR constellation ($M_{HR} = 16$ in Fig. 3). Thus the number of points within a cluster is given by $M_{cluster} = M_{HR}/M_{LR}$. This value combined with ϕ_1 determines the values ϕ_2 can take to avoid clusters overlapping. The possible values of ϕ_1 and ϕ_2 are given by the ratio:

$$\frac{\phi_2}{\phi_1} = \frac{\alpha}{M_{cluster}}, \tag{2}$$

where $0 < \alpha < 1$. It is also convenient to define $\theta = \phi_1 - \phi_2(M_{cluster} - 1)$ as shown in Fig. 3. α is the PSK-equivalent of λ from the QAM case in [6].

Now that the constellation parameters are described, the SER can be calculated in terms of the defined values. For receivers demodulating the HR constellation, the probability of symbol error is given by

$$\begin{aligned} SER_{HR} = \frac{1}{M_{HR}} \Bigg(& 2M_{LR}\left(P_{err}\left(\frac{E_s}{N_0}, \psi \geq \theta\right)\right. \\ & \left.+ P_{err}\left(\frac{E_s}{N_0}, \psi \geq \phi_2\right)\right) \\ & + (M_{HR} - 2M_{LR})2P_{err}\left(\frac{E_s}{N_0}, \psi \geq \phi_2\right)\Bigg), \end{aligned} \tag{3}$$

where $2M_{LR}$ is the number of points that are cluster edges, $M_{HR} - 2M_{LR}$ is the number of points that are not cluster edges, and $P_{err}\left(\frac{E_s}{N_0}, \psi >= \phi\right)$ is the angular probability of error given by $P_{err}\left(\frac{E_s}{N_0}, \psi >= \phi\right) = F(\frac{E_s}{N_0}, \pi) - F(\frac{E_s}{N_0}, \phi)$ from [9].

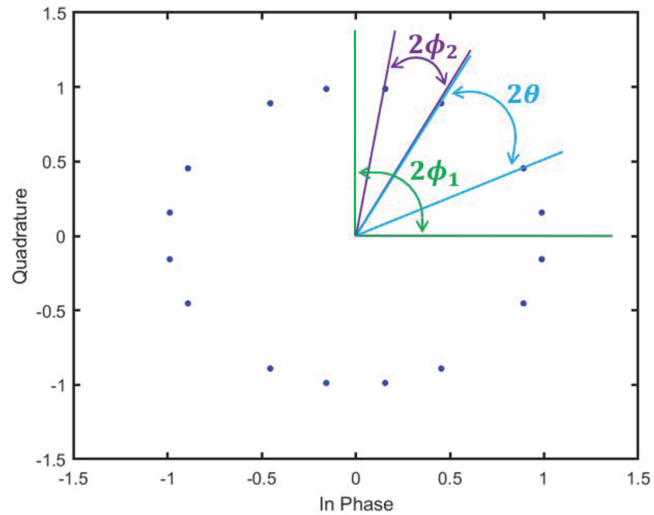

Fig. 3. Parameters for PSK HBM constellation

Receivers demodulating at the LR would experience an error rate given by

$$\begin{aligned} SER_{LR} = & \frac{2}{M_{cluster}^2} \\ & \Bigg(2M_{cluster}P_{err}\left(\frac{E_s'}{N_0}, \theta + \phi_2(M_{cluster} - 1)\right) \\ & + \Sigma_{m=1}^{M_{cluster}-1}\{m\Bigg(P_{err}\left(\frac{E_s'}{N_0}, \theta + \phi_2(m-1)\right) \\ & + P_{err}\left(\frac{E_s'}{N_0}, \theta + (2M_{cluster} - m - 1)\phi_2\right)\Bigg)\}\Bigg). \end{aligned} \tag{4}$$

Note that the energy per symbol for the LR receiver is given by E_s', and it is greater than the energy per symbol for the HR receiver E_s because the LR symbols last twice as long as the HR symbols if $k = 2$ and longer if $k > 2$.

We verified (3) and (4) by simulating a full end-to-end transmitter to receiver system in MATLAB. The results are shown in Fig. 4 for a 8/64 PSK HBM system with $\alpha = 0.8$. For both the LR and the HR, the theoretical and simulated values line up perfectly. Thus, the theoretical expressions provide a true characterization of the error rate for HBM PSK.

B. Functional Region

From expressions (3) and (4), we can determine which values of α will result in a successful HBM system. The HBM functional region is defined in [7] for HBM QAM systems as the region of λ values which correspond to both LR and HR SERs existing below a given threshold. A similar region can be defined for HBM PSK systems considering α.

In Fig. 3, it can be seen that $\alpha = 1$ corresponds to a uniform PSK constellation, and defining $\alpha > 1$ would result in overlapping clusters. Thus α must be less than or equal

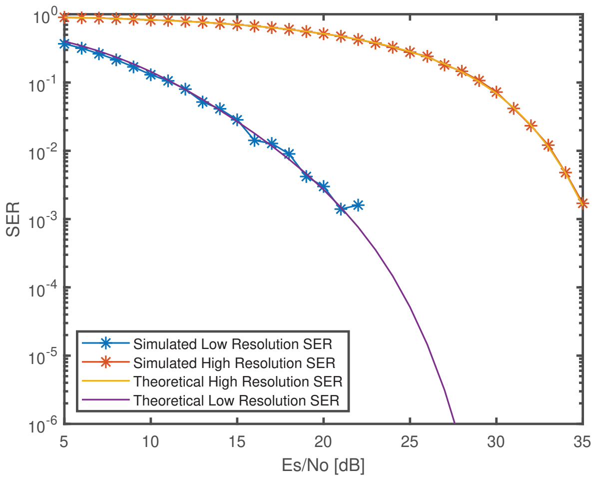

Fig. 4. SER for a 8/64 PSK HBM system with $\alpha = 0.8$

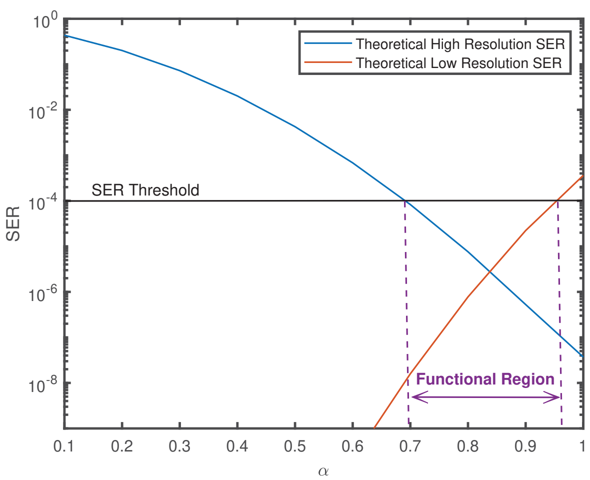

Fig. 5. SER as a function of α showing HBM PSK Functional Region

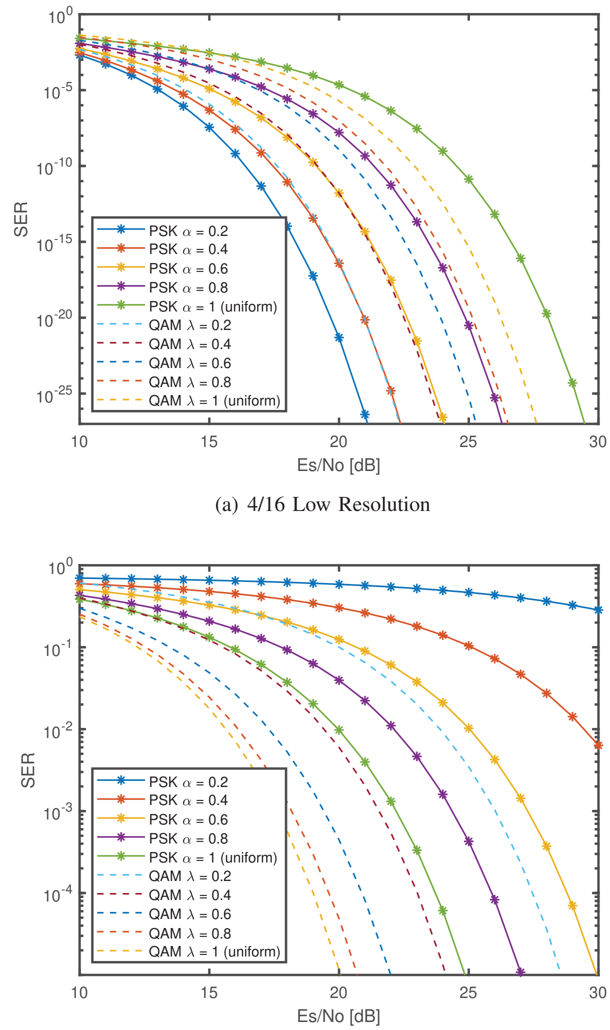

(a) 4/16 Low Resolution

(b) 4/16 High Resolution

Fig. 6. Error rates for PSK and QAM HBM Systems

to 1, but if α is too small, the HR receiver will struggle to demodulate the constellation. The ideal α will depend on the E_s/N_0 value at both receivers which depends on the transmission distance. (3) and (4) are functions of α, E_s/N_0, and SER. Thus, by performing a link budget analysis to determine the expected E_s/N_0 and E_s'/N_0 values for the near and far receivers, E_s/N_0 can be held constant, and SER can be plotted as a function of α for each receiver. An example is shown in Fig. 5 for a 4/16-PSK system with bandwidths of 10 GHz and 20 GHz for receivers observing E_s/N_0 values of 20dB and 26dB respectively. The HR SER strictly decreases with α because as α increases, the constellation approaches a uniform PSK for the HR receiver. Meanwhile the LR SER strictly increases with α because spreading points within a cluster appears as noise to the LR receiver.

Defining a required SER threshold, automatically introduces a range of α values that correspond to acceptable performance of both LR and HR systems. In our example in Fig. 5, we arbitrarily choose an uncoded SER threshold of 10^{-4} to demonstrate this property. The functional region in this example is given by $0.7 < \alpha < 0.97$. It is important to remember that these values of α are only viable for the specific scenario in which Fig. 5 was plotted. Thus if any parameters change (i.e. the E_s/N_0 values, the bandwidth, the modulation order, etc.), the functional region would move laterally, shrink, or expand. In order to design a successful HBM system, the functional region should be considered.

IV. Comparing HBM PSK and HBM QAM Performance for THz Systems

In this section we proceed to compare the error rates for the HBM PSK and QAM systems and their PAPR values to analyze their potential for THz systems.

The expected error rates as derived in [7] and in Sec. III-A are shown in Fig. 6. We see the high resolution error rates decrease as λ and α approach 1, which corresponds to a

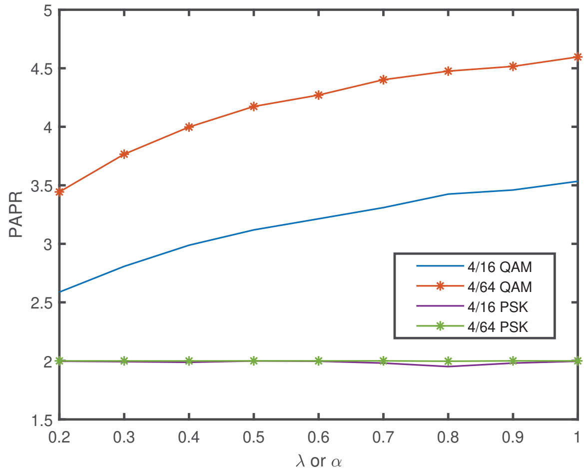

Fig. 7. PAPR of HBM signals using QAM and PSK constellations as a function of values of α (for PSK) or λ (for QAM)

uniform constellation. Meanwhile, the low resolution error rates increase as λ and α approach 1, because increasing λ and α results in added deviations from the expected low resolution symbols.

Comparing the PSK and QAM results, we can see that for small values of λ and α, the low resolution receiver performs better with PSK while the high resolution receiver performs better with QAM. Still it is important to remember that receivers demodulating the high resolution constellation would be observing a high SNR. Additionally, we must remember that THz radios will not operate optimally with constellations with a high PAPR.

As shown in Fig. 7, the PSK constellation provides a signal with a constant PAPR while the PAPR of QAM constellations increases with the modulation order. Thus in a PAPR-limited system, HBM PSK offers a feasible option to achieve higher data rates than traditional HM or non-hierarchical PSK without introducing a PAPR problem.

V. Experimental Results

A. Experimental Demonstration

The TeraNova testbed described in [10] was used to experimentally demonstrate a PSK HBM system using the parameters shown in Table I. The goal of this experiment was to demonstrate that the low resolution information can be fully recovered successfully at farther distances while the high resolution sent at a faster symbol rate information can be successfully recovered at short distances. The transmitted signal used a 8/16 PSK constellation and $\alpha = 0.5$. The HBM signal itself was designed in MATLAB with a HR symbol rate of 5 Gsps and a LR symbol rate of 2.5 Gsps. These corresponded to bandwidths of 10 GHz and 5 GHz as shown in Fig. 2. After being designed in MATLAB, this signal was uploaded to an arbitrary waveform generator (AWG), that converted it to an analog signal. It was mixed with a 130 GHz signal before radiating out of a 38 dBi antenna. On the receiver side, the signal was captured using a 21 dBi antenna before being mixed again with a 130 GHz signal to bring it back to baseband. After passing through a Low-Noise Amplifier, the signal was digitized by a Digital Storage Oscilloscope (DSO), before detection was performed in MATLAB. The transmitter and receiver were placed 6m apart to start, and then the distance was increased by 3m increments to capture the signals that would be seen by the near and far receivers. The signals captured at each distance were processed using both the HR and the LR demodulators in MATLAB, and the results are shown in Table II.

TABLE I
Experimental Parameters

Transmission Power	19 dBm
Tx Antenna Gain	38 dBi
Rx Antenna Gain	13 dBm
Carrier Frequency	130 GHz
HR Bandwidth	10 GHz
LR Bandwidth	5 GHz
α	0.5

TABLE II
Experimental Results for a 8/16 PSK HBM System

Distance [m]	Low Resolution SER	High Resolution SER
6	$< 8.33 * 10^{-4}$	$3.33 * 10^{-4}$
9	$< 8.33 * 10^{-4}$	0.0127
12	$< 8.33 * 10^{-4}$	0.0203
15	0.0093	0.2838

The HR receiver only has a low error rate at 6m, while the LR receiver can successfully demodulate until the distance increases to 15m. An example of the received constellations is also shown in Fig. 8. Notice that the HR receiver successfully demodulates all 16 constellation points in a non-uniform circle, while the LR receiver demodulates 8 clusters uniformly distributed.

VI. Conclusion

In this paper we have explored PSK HBM as a promising solution for single-carrier STMR systems. We have proved HBM's ability to outperform other STMR multiplexing techniques in terms of achievable capacity and have mathematically characterized the SER for PSK HBM systems. Our findings were verified with simulations, and experimental results show HBM as a tangible possibility for THz systems. Before HBM can be used, research determining optimal coding schemes for HBM systems should be performed as well as a deeper study to characterize the performance of the QAM HBM system. These topics will be explored in our future work.

Acknowledgments

This work was supported in part by the US Air Force Research Laboratory Grant FA8750-20-1-0200 and the US National Science Foundation Grant CNS-2011411. We would also like to thank Priyangshu Sen, Claire Parisi, Sergi Aliaga, and Jacob Hall for their feedback.

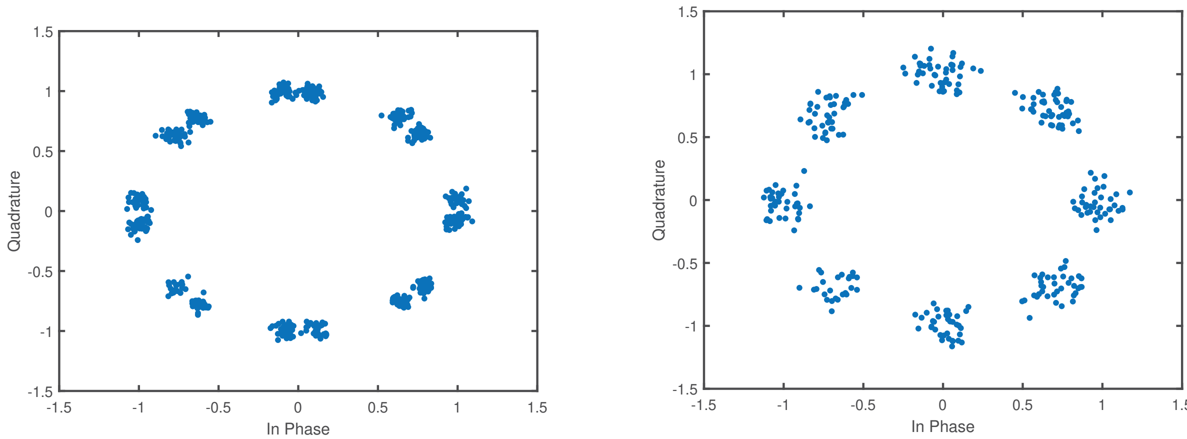

(a) High Resolution Receiver at 6m

(b) Low Resolution Receiver at 9m

Fig. 8. Received 8/16 PSK constellation with $\alpha = 0.5$

REFERENCES

[1] I. F. Akyildiz, C. Han, Z. Hu, S. Nie, and J. M. Jornet, "Terahertz band communication: An old problem revisited and research directions for the next decade," *IEEE Transactions on Communications*, 2022.

[2] K. Sengupta, T. Nagatsuma, and D. M. Mittleman, "Terahertz integrated electronic and hybrid electronic–photonic systems," *Nature Electronics*, vol. 1, no. 12, pp. 622–635, 2018.

[3] J. M. Jornet and I. F. Akyildiz, "Channel capacity of electromagnetic nanonetworks in the terahertz band," in *2010 IEEE international conference on communications*. IEEE, 2010, pp. 1–6.

[4] B. Ning, Z. Tian, Z. Chen, C. Han, J. Yuan, and S. Li, "Prospective beamforming technologies for ultra-massive mimo in terahertz communications: A tutorial," *arXiv preprint arXiv:2107.03032*, 2021.

[5] X. Ma, Z. Chen, W. Chen, Y. Chi, Z. Li, C. Han, and Q. Wen, "Intelligent reflecting surface enhanced indoor terahertz communication systems," *Nano Communication Networks*, vol. 24, p. 100284, 2020.

[6] Z. Hossain and J. M. Jornet, "Hierarchical bandwidth modulation for ultra-broadband terahertz communications," in *ICC 2019-2019 IEEE International Conference on Communications (ICC)*. IEEE, 2019, pp. 1–7.

[7] D. M. Bodet, P. Sen, Z. Hossain, N. Thawdar, and J. M. Jornet, "Hierarchical bandwidth modulations for ultra-broadband communications in the terahertz band," *to appear in IEEE Transactions on Wireless Communications*, 2022.

[8] H. Jiang and P. A. Wilford, "A hierarchical modulation for upgrading digital broadcast systems," *IEEE transactions on broadcasting*, vol. 51, no. 2, pp. 223–229, 2005.

[9] R. Pawula, S. Rice, and J. Roberts, "Distribution of the phase angle between two vectors perturbed by gaussian noise," *IEEE Transactions on Communications*, vol. 30, no. 8, pp. 1828–1841, 1982.

[10] P. Sen and J. M. Jornet, "Experimental demonstration of ultra-broadband wireless communications at true terahertz frequencies," in *2019 IEEE 20th International Workshop on Signal Processing Advances in Wireless Communications (SPAWC)*. IEEE, 2019, pp. 1–5.